

USE OF INSULATED IRON POWDERS IN A BICYCLE PERMANENT MAGNET ELECTRIC MOTOR

C. Gélinas¹, J. Cros², L.-P. Lefebvre³, A. St-Louis⁴ and J.-Y. Dubé⁵

- 1. Quebec Metal Powders Limited, Sorel-Tracy, Québec, Canada**
- 2. Laval University, Ste-Foy, Québec, Canada**
- 3. Industrial Materials Institute/NRCC, Boucherville, Québec, Canada**
- 4. Maxtech Powder Metal, Ste-Foy, Québec, Canada**
- 5. Energy Propulsion System, Asbestos, Québec, Canada**

ABSTRACT

Insulated iron powders are gaining acceptance as alternative materials to steel sheet laminations used in electrical motors. This is being driven by the potential for reduced costs, reduced parts per component, and increased design flexibility due to the isotropic nature of the iron composite materials. Here a systematic approach was used to design an original permanent magnet electric motor integrating an iron composite stator.

In the paper are described the different steps involved in the development of this stator. From the first design iterations, to the prototype testing, trials on an industrial press and production. The focus is put on the design, materials and compaction aspects.

INTRODUCTION

Traditionally, steel laminations are used as soft magnetic materials in electrical motors. There are now available iron-based powders specifically engineered for magnetic applications in alternating fields called soft magnetic composites or SMC. These materials possess isotropic properties that give end users and designers the possibility to make motors with a topology more adapted to the final application. Although SMC have lower maximum permeability and magnetic induction than laminations, there are electrical machines which can take advantage of their benefits. For instance, permanent magnet motors are amongst the most appropriate applications for the use of SMC. Indeed, in these structures, this is the high reluctance of the mechanical air gap and magnets that dominates the effective magnetic circuit, not the reluctance of a SMC stator.

Another interesting feature of the SMC, that played an important role in the realization of the present project, is the ease of prototyping. A privileged approach in the feasibility study of a given project, consists in modeling of the application and then building of a prototype by machining a larger workpiece of pressed SMC. This is the approach that was used to demonstrate the feasibility of

using a SMC stator in an electric motor for a bicycle. In the present case, the success achieved in the first part of the project eventually conducted to the manufacturing of the electric motor through conventional tool and die compaction.

The different steps involved in the development of the SMC stator, from the first design iterations, prototype testing and production on an industrial press are presented.

MOTOR DESIGN MODELING & TESTING

The main constraints of an electrical bicycle drive system are the cost and weight minimizations. However, the total efficiency, the starting torque and the torque ripple are also important factors of the performance of a drive system [1]. Table I shows some specifications of this application.

Table I. Main specifications of the electric bicycle motor.

Continuous power	240 W
Peak power	650 W
Maximal speed	32 km/h
Total weight (without battery)	Less than 4 kg
Battery DC voltage	24 V
Main design objectives	Maximize efficiency Minimize cost & weight

There are two kinds of drive methods used in electrical bicycle applications: the indirect drive approach or the direct drive approach. In the first approach, a speed reducer (belt or gear) is added to minimize the motor size but the efficiency is degraded. In the second approach, a direct drive low speed permanent magnet motor and the power electronic stage are mounted in the wheel [2,3]. In the present case, this is the direct drive approach with a specific structure of brushless DC motor and control system that was chosen to improve the efficiency and to minimize the battery size.

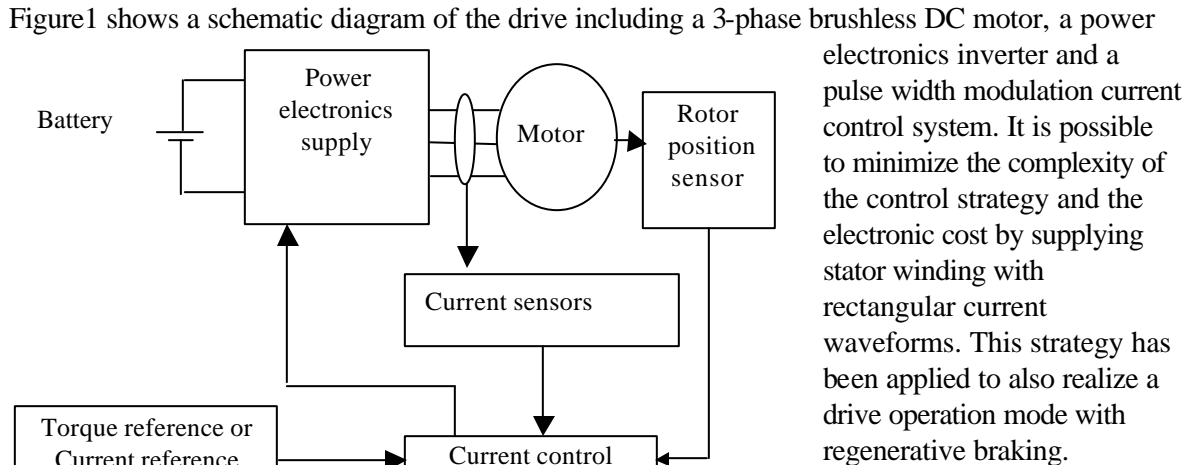


Figure 1. Brushless DC motor for variable speed drive application.

The selected motor has a radial airgap and outer rotor structure. There are 24 stator slots and 22 rotor poles made of sintered NdFeB permanent magnets glued on the surface of a massive iron yoke. The stator magnetic circuit could be realized with a SMC or a laminated material. SMC have a lower permeability than conventional laminated materials that usually reduces the torque performance. However, this drawback is minimized in magnetic circuits comprising permanent magnets because the length of the intrinsic distributed air gap of the SMC is much lower than the length of the total air gap of the device [4]. Also, SMC have isotropic magnetic and thermal properties and because the magnetic flux can circulate in three dimensions, it is possible to perform a flux concentration in the magnetic circuit of the stator winding in the axial direction. In this case, the tips of the teeth can be axially expanded for an air-gap flux concentration into the teeth and the yoke of the stator. It can be an interesting advantage in the case of the use of ferrite permanent magnets where the air-gap flux density is low [3,4]. The total axial length of the motor is then minimized without decreasing the performance. However, this approach provides a small improvement when high energized NdFeB permanent magnets are used.

The selected stator structure has a specific 3-phase concentrated winding with coils directly wound around the teeth [4,5]. This winding configuration is easier to realize than a lap winding and reduces the copper volume of the end-windings, the copper losses and the total axial length of the motor. An armature concentrated winding structure has also a small number of slots having relatively large dimensions. Consequently, this structure is well adapted to the realization of the magnetic circuit with a SMC material. The mechanical constraints on the molding device are reduced and the pressing process is easier.

The design of the motor has been achieved by use of analytical design models and evaluated using field calculation tools to optimize its performance. Figure 2 shows the magnetic flux density distribution in a transversal section of a SMC structure in the case of a maximal torque operation. A first validation prototype has been realized by machining pre-pressed ATOMET EM-1 slugs. This first prototype or demonstrator is shown in Figure 3. On the left, can be seen the NdFeB permanent magnets glued on the internal surface of the rotor and on the right, the machined SMC stator with the concentrated copper windings.

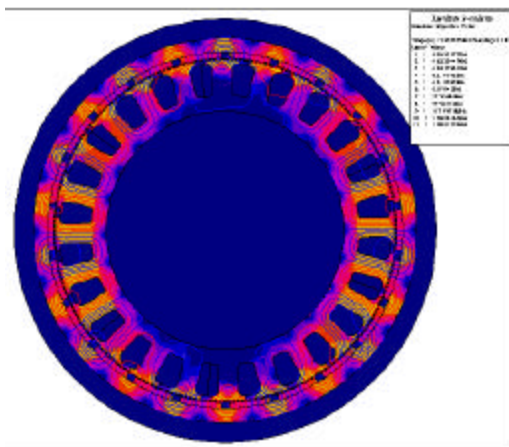


Figure 2. Flux density distribution at the maximal torque operation.

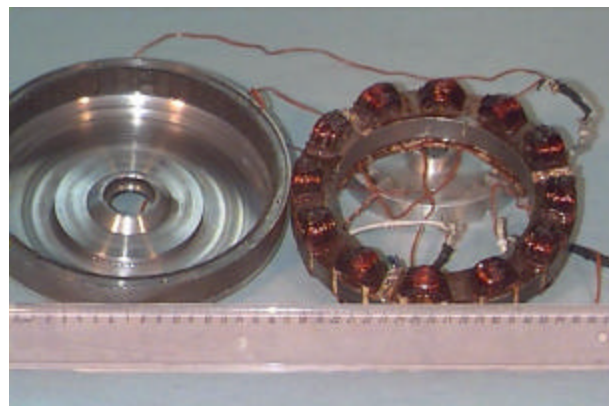


Figure 3. First prototype with the rotor (left) and machined SMC stator (right).

Table II gives some experimental results measured on this demonstrator. With such a concentrated winding structure, one can see that the electrical resistance is low and that the copper losses are acceptable for the rated continuous operation point. The cogging torque is also low without stator slot skewing. In the case of ATOMET EM-1, the magnetic losses are mainly hysteresis losses proportional to frequency or speed. For this application and for such a motor, these losses are not really important when compared to the copper losses at the rated operation point but they add a constant drag torque independent of the speed.

Table II. SMC motor characteristics.

Number of stator slots	24
Number of rotor poles	22
Copper weight	0.87 kg
NdFeB Magnet weight	0.25 kg
Weight of stator magnetic circuit	1.54 kg
Concentrated winding	12 coils with 28 turns
Single phase electrical resistance	66 mohm
Maximal no-load speed (24V DC supply)	350 rpm
Rated continuous output torque	7.8 N.m – 11.8 A
Cogging torque	< 0.4 N.m
Operation with $P_{out} = 250$ W at 300 rpm	
Joule losses	18 W
Magnetic losses	< 8W
Constant torque of hysteresis losses	< 0.4 N.m
Motor efficiency	88.6 %

It is worth noting that specific advantages of the SMC materials for electrical machine design were not used in this particular application. For instance, the isotropy of the SMC magnetic and thermal properties was not exploited. The scope of the modeling work was really to meet the original objective of demonstrating the feasibility of using a SMC stator in the manufacturing of an electric motor.

SMC MATERIALS ASPECTS

SMC are ferromagnetic powders insulated from each other by a thin organic or inorganic film. This thin film acts primarily as an electrical barrier to reduce or suppress Eddy currents in AC applications and also as a mechanical strengthener after consolidation by pressing and heat treating at low to moderate temperatures. The use of high purity water-atomized iron particles provides the high compressibility required to achieve high density and magnetic properties. The quantity of organic compounds is kept as low as possible in order to get the best performance from the ferromagnetic properties of iron.

Two types of SMC materials are manufactured by QMP that cover the low to medium frequency range of applications. ATOMET EM-1 is an iron-resin material system which requires lubrication of

the die walls during compaction. After pressing, parts are cured at low temperature (200°C to 325°C) in air to cross-link the resin and achieve high strength. ATOMET EM-2 is an iron-dielectric material in which the dielectric acts as a lubricant during the compaction as well as an insulator after a moderate temperature heat treatment (typically 350°C to 500°C). Some characteristics of these composite materials are given in Table III. The two materials are complementary in terms of electrical resistivity which is governed by the amount of insulating material and temperature of the heat treatment. While ATOMET EM-1 can be used in a very large range of frequency applications, ATOMET EM-2 is rather intended for applications below 400 Hz and particularly suitable for pressing complex shapes.

Table III. Characteristics of the ATOMET EM-1 and EM-2 materials used for low to medium frequency applications.

Material	ATOMET EM-1	ATOMET EM-2
Description	Iron-resin	Iron-dielectric
Apparent density	2.80 g/cm ³	3.00 g/cm ³
Hall flow rate	28 s/50 g	28 s/50 g
Compaction	External lubrication	Conventional
Curing (30 min)	200 - 325°C	350 - 500°C
Resistivity	200 - 500 μohm-m	10 - 100 μohm-m
Applications	50 - 20000 Hz	50 - 400 Hz

The mechanical and magnetic properties of such dielectromagnetics are dependent on the density and heat treatment temperature, similar to any other powdered metal part. Some properties for ATOMET EM-1 cured at 200°C and ATOMET EM-2 treated at 350°C are presented in following sections.

For instance, the compressibility of the two composite materials, as obtained by pressing transverse rupture (TR) bars, is illustrated in Figure 4. They exhibit a very similar compressibility behavior with the ATOMET EM-2 being slightly more compressible in the intermediate compacting pressure range.

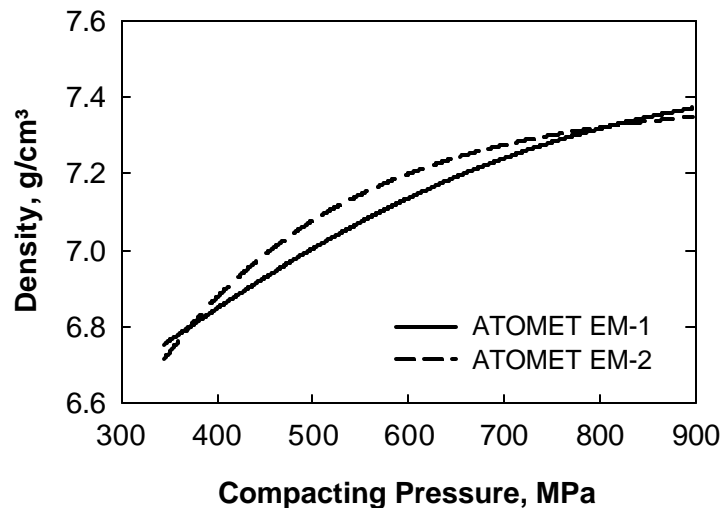


Figure 4. Effect of compacting pressure on the density of TR bars pressed from two SMC materials.

The mechanical strength of these SMC materials after their respective heat treatment is illustrated in Figure 5 as a function of the density. The ATOMET EM-1 iron-resin material exhibits the highest values, up to 125 MPa at a density of about 7.20 g/cm³. The strength of ATOMET EM-2 iron-dielectric material is more density-dependent and values as high as 110 MPa at densities above 7.20 g/cm³ can be reached. For this material, it is also possible to resin impregnate the low density parts (below 7.0 g/cm³) in order to increase the strength to values of about 100 MPa [6].

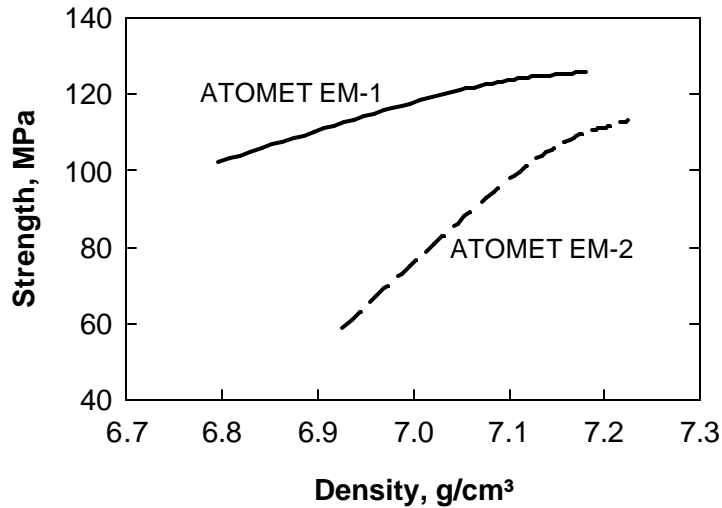


Figure 5. Effect of density on the mechanical strength of TR bars pressed from two SMC materials.

The effect of density of ATOMET EM-1 and EM-2 materials on the magnetic induction is presented in Figure 6. Magnetic properties were measured at an applied field of 120 A/cm (150 Oe) on toroids 5.26 cm OD by 4.34 cm ID by 0.635 cm thick. The induction is proportional to the density and not greatly affected by the mix formulation. In fact, there is a linear relationship between the density of these materials and their magnetization that can be expressed by the following equation : $B_{120} = (5.11 * \text{Density}) - 23.16$ where B is expressed in kGauss.

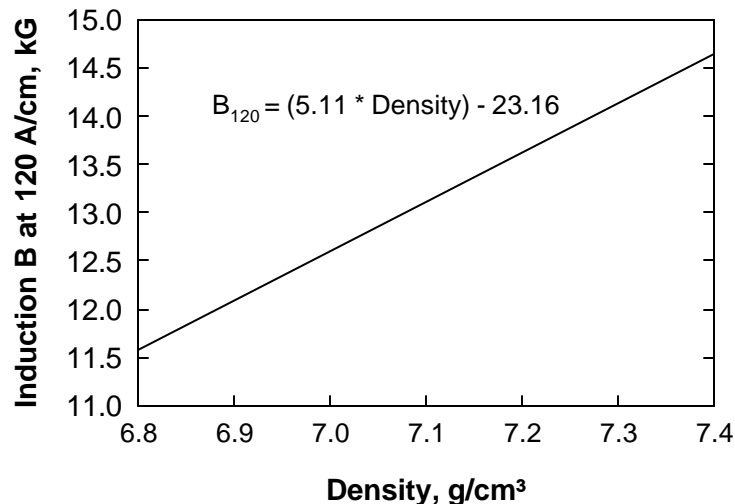


Figure 6. Effect of density of SMC materials on the magnetic induction at an applied field of 120 A/cm.

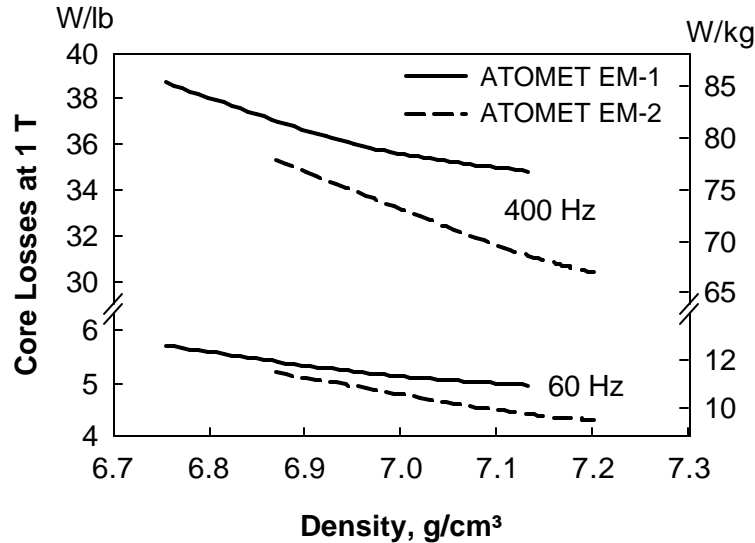


Figure 7. Effect of density on the total core losses at 1 Tesla measured at 60 and 400 Hz.

The effect of the density on the AC losses at 1 Tesla measured at 60 Hz and 400 Hz for these SMC materials is presented in Figure 7. The AC losses decrease with an increase in density that can be attributed to a decrease in the hysteresis loss. Indeed, with powdered materials, as the density increases magnetization becomes easier because of the resulting higher magnetic induction, higher permeability and lower coercive force. This improvement in DC characteristics with an increase in density translates into a decrease of the hysteresis portion of the core loss.

The iron-dielectric ATOMET EM-2 material shows losses approximately 12% lower than for ATOMET EM-1. This is due to the 350°C heat treatment that slightly reduces the hysteresis loss in this material. Indeed, hysteresis losses are relatively high in SMC and a heat treatment has a beneficial effect on their magnetic properties, even at a temperature as low as 350°C [6,7,8]. For these materials at densities above 7.0 g/cm³, losses are about 10 W/kg at 60 Hz and 70 W/kg at 400 Hz. The fact that the AC losses are proportional to the frequency and not to the square of the frequency, is a good indication that the insulation is efficient and eddy currents remain low, even in ATOMET EM-2 which has a lower resistivity.

PROTOTYPING & PRODUCTION

Following the successful testing of the demonstrator with a SMC stator, the prototyping process followed during which a tooling was designed and built for the compaction, motors were assembled and bicycles field tested.

The unique distributed air gap characteristic of the SMC makes that sectioning a SMC structure in few parts, creating supplementary air gaps, does not affect the overall flux carrying capacity. This characteristic allowed the SMC stator to be splitted in 4 parts or segments, one of them being shown in Figure 8, permitting the use of a 150 ton mechanical press for the compaction (Figure 9). The modular design of the segments with their male and female grooves on the contour eases the rotor assembly. It is also possible to stack them for the production of more powerful motors. The

low frequency of application (≈ 50 Hz) and reduced mechanical strength requirement resulting from the splitting in 4 parts made that the press-ready ATOMET EM-2 powder could be used in this application. The mix was compacted in automatic mode into 20 mm thick stator segments at a rate of 5 parts per minute. The compaction and ejection characteristics as well as the stability of the compaction process were evaluated during the production of the stator segments.

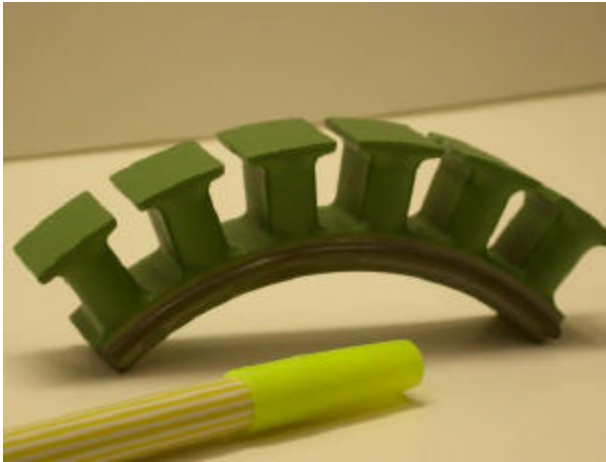


Figure 8: Stator segments compacted during the prototyping phase.



Figure 9 : Mechanical press used in the prototyping.

The density of the 20 mm thick stator segments as a function of the compacting pressure is

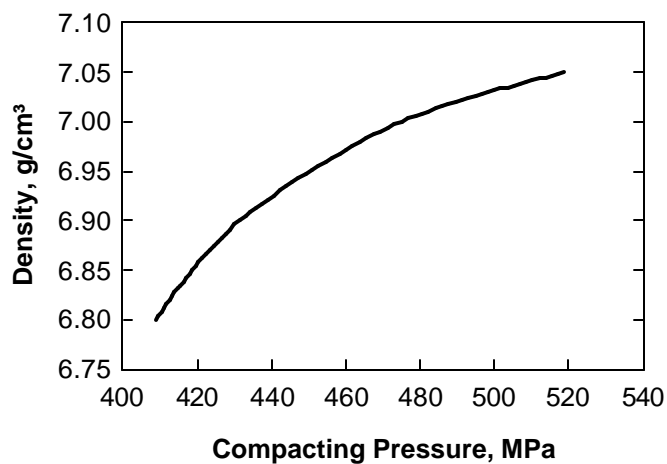


Figure 10. Effect of compacting pressure on the density of 20 mm thick stator segments.

illustrated in Figure 10. Similarly to any conventional P/M parts, the density is slightly lower than the one predicted from standard TRS bars (fig. 4) due to the thickness and complexity of the components. The friction surface in contact with the die is significantly higher than that of standard TRS bars (54.3 cm^2 for the stator segment vs 2.2 cm^2 for TRS bars). The friction between the powder and the surface of the die during compaction causes a pressure drop along the part and affects the final density of the components.

Variations in part weight during a production run gives an indication of the product consistency. In Figure 11 is plotted the part weight of stator segments pressed at a density of 6.85 g/cm^3 during a short production run. An average weight of 274.23 g was obtained with a total weight variation of less than 1.6 g (6 sigma). This indicates that the powder flowability, processing conditions and filling of the die cavity were good for this relatively complex part geometry.

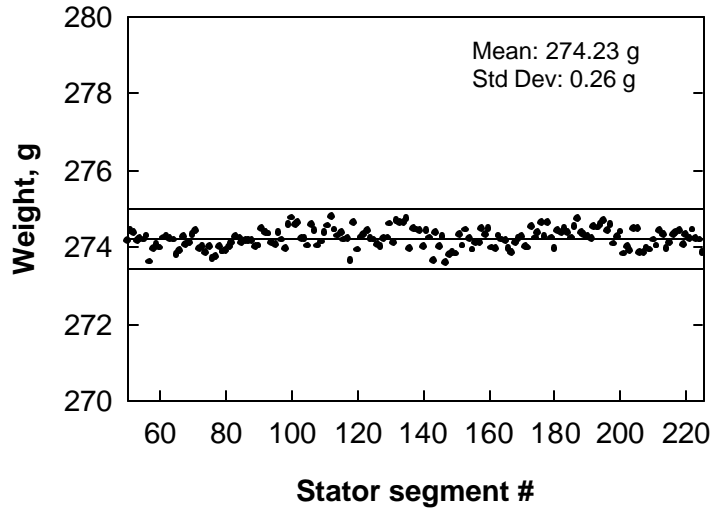


Figure 11. Weight variation of the stator segments (lines stand for the mean \pm 3 std dev).

The ejection of the components was smooth and relatively low ejection pressures were recorded (calculated by dividing the ejection shear stress by the surface of the part in contact with the die walls). The ejection curves taken at every 50 parts and reported in Figure 12 show that the ejection behavior remained stable all along the production run.

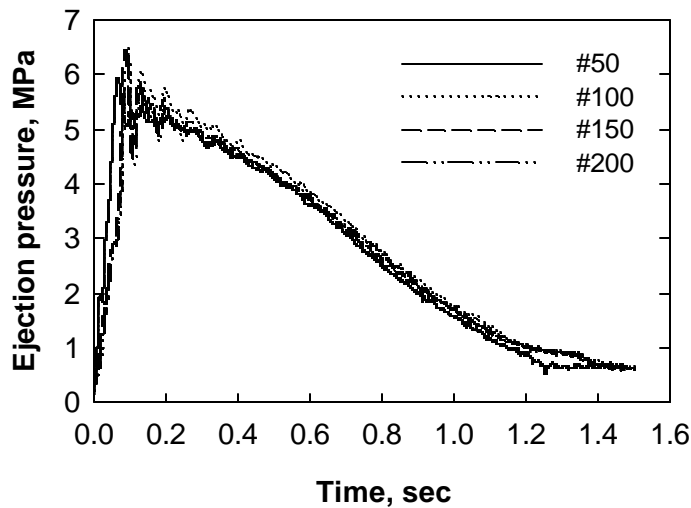


Figure 12. Ejection curves taken during the production of 20 mm stator segments pressed at 6.85 g/cm^3 (5 parts/min).

The first motors produced during this prototyping phase were submitted to laboratory and field testings. The electronics, assembly and control aspects of the assisted electric bicycle were optimized in order to give the rider a pleasant feeling. The final SMC stator part mounted on an aluminum hub with an internal cavity provided for the insertion of the electronic components is shown in Figure 13. Aluminum flanges are used to secure the SMC stator parts and ease the winding.



Figure 13. Final SMC stator comprising four segments inserted between two aluminum flanges.

Once this successful prototyping phase completed, the tooling for the compaction of the stator segments was transferred to Maxtech Powder Metal for the manufacturing. And after few production runs, the first commercial bicycles went into market. One of these bicycles is shown in Figure 14. The motor is mounted in the rear wheel, the battery pack on the inferior bar of the bicycle and the command console on the handle bar. The sophisticated electronics provide the rider with four levels of assistance (from 25% up to 200%) and a regenerative mode that can recharge the battery while cycling, braking or going down steep hills.



Figure 14. Assisted electric bicycle with the motor mounted in the rear wheel.

CONCLUSION

The success of this project, initiated in 1998, is another example of the potential of the SMC technology for electric motor applications from the early steps of material and motor design to production and commercialization. This valuable experience helped demonstrate the need for the development of multidisciplinary expertise and collaboration between material scientists, electrical and mechanical designers, part makers and industry partners, crucial for this emerging technology. It is obvious that specific advantages of the SMC materials for electrical machine design have not been systematically exploited in the early design steps of this particular application. For example, the motor structure was not using the isotropy of the SMC magnetic and thermal properties. It was also not optimally adapted to the production constraints and advantages of powder metallurgy like the simplification of the assembly and the winding realization. However, this project aided in the development and refinement of analytical design models and field calculation tools adapted to 3D

designs. Improvements in material processing (formulation, pressing and curing) and their integration into the new concepts in the assembly of electrical motors (modular stator parts, concentrated windings, ...) were realized.

Since then, new concepts were developed such as the integration of the thermal, electromagnetic and mechanical properties (unique to SMC) being employed in a single “global design”. They have been illustrated in several recent publications where comparative analysis between the conventional laminated technology and the SMC technology was made on a same application [4,10,11,12,13]. And as with any advancement in a technology, education is of prime importance. In the case of SMC materials, education is not restricted to just the magnetic component designer. Both the powdered metal parts makers and the end users must understand the advantages and limitations of SMC materials when compared to a conventional laminated steel material.

REFERENCES

1. H. Oman, W.C. Morchin, F.E. Jamerson, “Electric -bicycle propulsion power”, WESCON’95, 7-9 Nov. 1995.
2. T.F. Chan, Lie-Tong Tan, Shao-Yuan Fang, “In-wheel permanent-magnet brushless DC motor drive for an electric bicycle”, *IEEE Transactions on Energy conversion*, Vol.17, June 2002, p229-233.
3. A. Muetze, A. Jack, B. Mecrow, “Brushless-DC motor using soft magnetic composites as a direct drive in an electric bicycle”, European Power Electronic EPE’2001, Graz, Austria, 27-29 August 2001.
4. J. Cros, P. Viarouge, Y. Chalifour, C. Gélinas, “Small brush DC motors using soft magnetic composites for 42V automotive applications”, Society of Automotive Engineers World Congress. SAE’03, paper 03M-275, Detroit, March 2003.
5. J. Cros, P. Viarouge, “Synthesis of high performance PM motors with concentrated windings”. *IEEE Transaction on Energy Conversion*, Vol.17 No2, June 2002 p248–253.
6. L.P. Lefebvre, C. Gélinas & P.E. Mongeon, "Consolidation of a lubricated ferromagnetic powder mix for AC soft magnetic applications", *Advances in Powder Metallurgy & Particulate Materials - 2002*, MPIF Princeton, NJ, pp 14-86 to 14-97.
7. L.P. Lefebvre, S. Pelletier & C. Gélinas, "Iron compacts for low frequency AC magnetic applications: Effect of thermal treatments", *Advances in Powder Metallurgy & Particulate Materials - 1998*, MPIF Princeton, NJ, pp 8-47 to 8-59.
8. C. Gélinas, F. Chagnon, S. Pelletier & L.P. Lefebvre, "Effect of curing conditions on properties of iron-resin materials for low frequency AC magnetic applications", *Advances in Powder Metallurgy & Particulate Materials - 1998*, MPIF Princeton, NJ, pp 8-3 to 8-11.
9. C. Gélinas, “Soft ferromagnetic powders for AC magnetic applications”, Workshop on Production and Applications of Soft Magnetic Materials for Electric Motors, Proc. Euro PM2000, EPMA, pp 1-8.

10. J. Cros, P. Viarouge, "New structures of polyphase claw-pole machine", *IEEE Transaction on Industry Applications*, Vol.40, No1, Jan/Feb 2004 p113, 120.
11. J. Cros, P. Viarouge, Y. Chalifour, J. Figueroa , "New structure of universal motor using soft magnetic composites", *IEEE Transaction on Industry Applications*, Vol.40, No2, March/April2004 p 550, 557,
12. J. Cros, A. J. Perin, P. Viarouge, "Soft magnetic composites for electromagnetic components in lighting applications", IEEE IAS'02 Annual Meeting, Vol.1, 13-18 Oct. 2002, p 342 – 347.
13. P. Viarouge, J. Cros, Y. Chalifour, C. Gélinas, "New structures of brush and brushless DC motors using soft magnetic composites for automotive applications", Society of Automotive Engineers World Congress. SAE'01, paper 2001-01-400, Detroit, 5-8 mars 2001.